

ON THE TRANSONIC FLOW PAST THIN AIRFOILS

Thesis by

Julian D. Cole

A handwritten signature in cursive script that reads "Julian D. Cole". The signature is written in black ink and is positioned below the printed name.

In partial Fulfillment of the Requirements for the Degree of
Aeronautical Engineer

California Institute of Technology
Pasadena, California

June 9, 1946

ACKNOWLEDGMENTS

The author wishes to thank Dr. Hans W. Liepmann for directing the research and giving essential assistance, Dr. Paco Lagerstrom for valuable discussions, and Harry Ashkenas for cooperation especially in obtaining experimental results.

TABLE OF CONTENTS

<u>Part</u>	<u>Title</u>	<u>Page</u>
I	Introduction	1
II	Application of Fourier Integral to the General Problems	5
III	Some Results and Comparison with Experiments	18

INTRODUCTION

This research was undertaken as part of a general program of the investigation of the formation of shock waves on airfoils. Consequently, it was thought advisable to study potential solutions for transonic flow to obtain information concerning the occurrence, size, and shape of supersonic zones. From this point of view it is especially desirable to include the effect of wind tunnel walls in modifying the flow field since the most reliable data can be obtained in wind tunnels.

Until recently the main methods of investigating transonic flow were:

(1) Expansion of the velocity potential in a double power series of space coordinates. This method, as applied by Taylor (Ref. 1) and Gortler (Ref. 2), solves an exact equation for the flow with approximate boundary conditions. Since the area of convergence is very limited the use of this method is restricted to local problems such as the flow in the throat of a nozzle, etc.

(2) Solution of the Hodograph Equation. The equation for the two-dimensional flow of a compressible fluid may be linearized by a transformation of the independent variables. (See Ref. 3) Then, in general, the simplified equation must be solved with correspondingly more difficult boundary conditions. Tsien and Kuo (Ref. 4) have applied this method to the flow past bodies of nearly circular shape, but even here the computations were lengthy.

(3) Development of velocity potential in power series of thickness ratio. In the first approximation this is the so-called "small perturbation" or Prandtl-Glauert method and has been used by many authors to obtain information about compressible flows. The first approximation is relatively simple and where carefully considered yields much information, even in transonic flow. Gortler obtained supersonic regions in the flow past a wavy wall in Ref. 8. The second approximation is more complex and has only been worked out for special cases, e.g. Hantzche and Wendt (Ref. 5). (For a ^{handwritten} revision of these methods see Ref. 3)

(4) Solution of an Approximate Transonic Equation. If in the two-dimensional, irrotational, isentropic flow of a compressible fluid,

a = velocity of sound at a point x, y in space

u = velocity of flow in x -direction at that point

v = velocity of flow in y -direction at that point,

$$(a^2 - u^2) \frac{\partial^2 \phi}{\partial x^2} - 2uv \frac{\partial^2 \phi}{\partial x \partial y} + (a^2 - v^2) \frac{\partial^2 \phi}{\partial y^2} = 0 \quad (1)$$

Then, u is considered to be only slightly different from a velocity of sound and v is considered to be small, i.e.,

$$u = a^* + \frac{\partial \phi}{\partial x} \quad \text{say}$$

$$v = \frac{\partial \phi}{\partial y}$$

where $\frac{\partial \phi}{\partial x}$ and $\frac{\partial \phi}{\partial y}$ are much less than u , so that squares of their ratio may be neglected and where $a^* =$ velocity of sound when it equals the flow velocity on $a^{*2} = u^2 + v^2$, Eq. (1) may be written

$$\frac{\gamma+1}{2} \frac{\partial \phi}{\partial x} \frac{\partial^2 \phi}{\partial x^2} + \frac{2}{a^*} \frac{\partial \phi}{\partial y} \frac{\partial^2 \phi}{\partial x \partial y} - \frac{\partial^2 \phi}{\partial y^2} = 0 \quad (2)$$

Solution of this equation should apply to transonic flow. Recently, E. Graham and Th. von Karman have used Eq. (2) as a starting point and have, by similarity methods, obtained some results for the drag of these bodies in transonic flow.

A consideration of the methods available made a logical first choice the application of the small perturbation theory to the transonic flow past airfoils. The small perturbation theory makes the solution of the flow of a compressible fluid an affine transformation of the solution of the flow of an incompressible fluid. The resulting problem in potential theory is solved by means of a Fourier integral. It can then be expected that as long as the assumptions made in the theory are not violated, the results will approximate the true flow. In this way, supersonic regions over an airfoil and wind tunnel wall effects can be considered.

When exact equations, like (1), are used, supersonic flow is governed by a hyperbolic equation and subsonic flow by an elliptic equation, or one can say that a supersonic zone is an hyperbolic region and a subsonic zone is an elliptic region. The linearized equation (see Eq. 5) used in the solution is, however, elliptic for all space. This implies the analytic continuation of an elliptic solution through a hyperbolic region. (The problem in general was devised by H. Bateman, Ref. 7). However, this is not too strange, for the limited hyperbolic region of a finite supersonic zone behaves elliptically, i.e., every point on it influences every other point and in fact, every point in space. This occurs in the following way:

Fig. 1, the influence of a disturbance or pressure pulse at B is felt in the domain downstream through B. Thus, the influence

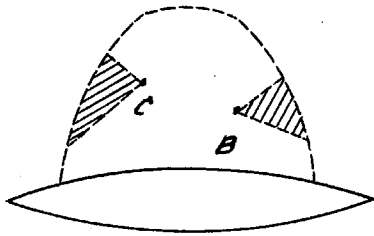


Fig. 1

of B is felt in the boundary of the elliptic region and affects the rest of the elliptic region and especially that part of the boundary in whose domain of influence C lies.

Physically, the small perturbation approximations are interesting for it will be noticed that stream tubes have no throat at sonic speed nor do they diverge when the velocity becomes supersonic. However, this is a natural consequence of replacing the exact equation for a stream tube, $(1 - M^2) \frac{du}{u} = -\frac{\Delta A}{A}$ where $M = \text{Mach number} = \frac{u}{a}$

$A = \text{area of stream tube}$

by an approximate one

$$(1 - M^2) \frac{\Delta u}{u} = -\frac{\Delta A}{A} \quad \text{where } M = \text{Mach number far from}$$

disturbance, as, in effect, the theory does.

II

APPLICATION OF SMALL PERTURBATION METHOD TO TRANSONIC FLOW

By considering the conservation of mass, energy, and momentum in a perfect compressible fluid which is disturbed only slightly from steady rectilinear flow, it is possible to describe the motion by the following linearized equation:

$$(1 - M_{\infty}^2) \frac{\partial u'}{\partial x} + \frac{\partial v'}{\partial y} + \frac{\partial w'}{\partial z} = 0 \quad (3)$$

where M = Mach number in the undisturbed stream $= \frac{V}{a_{\infty}}$
 if V = velocity of flow in free stream, taken parallel to x-axis
 and a_{∞} = varied velocity in free stream

Also, if u, v, w are the velocity components at a point x, y, z in the x, y, z direction respectively, then the induced velocities

$$u' = u - V$$

$$v' = v$$

$$w' = w.$$

In the diameter of B it is assumed that the induced velocities are small compared to the free stream velocity so that squares of this ratio may be neglected and that $\frac{t}{V} \frac{\partial u'_i}{\partial x_k}$ is also small, where t = a characteristic length of the body causing the disturbance, u'_i is any induced velocity, and x_k is any coordinate. (See Ref. 1) These assumptions must be later checked. It can also be shown, using the same approximation that the pressure coefficient

$$C_p = \frac{p - p_{\infty}}{\frac{1}{2} \rho_{\infty} V^2} = - \frac{2u'}{V} \quad \text{when } p \text{ denotes pressure and } \rho \text{ density.} \quad (4)$$

If the free stream has subsonic velocity and the entire motion can be considered two dimensional,

$$\beta^2 \frac{\partial^2 \phi}{\partial x^2} + \frac{\partial^2 \phi}{\partial y^2} = 0$$

where ϕ is a perturbation (5)

potential such that

$$u' = \frac{\partial \phi}{\partial x}$$

$$v' = \frac{\partial \phi}{\partial y}$$

$$\beta^2 = 1 - M_{\infty}^2 > 0$$

Some solutions of (3) in special cases are now given.

A. Flow past a wall of almost arbitrary shape, the medium extending to infinity y , as in Fig. 1, x, y are the coordinates in a physical plane and $y = f(x)$ gives the shape of the wall, then (3) must be solved with certain boundary conditions. These are:

1. No disturbance in y -direction far from the wall on

$$(6) \quad v' = \frac{\partial \phi}{\partial y} \rightarrow 0 \quad y \rightarrow \infty$$

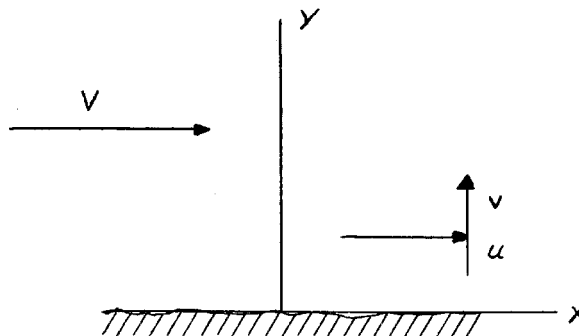
and

2. Flow tangent to the wall.

Within the approximation of the theory this can be expressed as:

$$(7) \quad \psi(x, 0) = V f'(x) \quad , \text{ i.e., the boundary condition}$$

is applied on the x -axis.



Now let $\xi = x$ so that
 $\eta = \beta y$

(8) $\phi_{\xi\xi} + \phi_{\eta\eta} = 0$ with these boundary conditions

1a. $\frac{\partial \phi}{\partial \eta} \rightarrow 0$ as $\eta \rightarrow \infty$

2a. $\frac{\partial \phi}{\partial \eta} = \frac{V}{\beta} f'(\xi)$ as $\eta = 0$

Then the solution may be written (if $f'(t)$ is suitably restricted).

(9)
$$\phi = -\frac{V}{\beta\pi} \int_0^{\infty} \frac{d\lambda}{\lambda} \int_{-\infty}^{\infty} e^{-\lambda\eta} f'(t) \cos \lambda(t-\xi) dt$$

for $\frac{\partial^2 \phi}{\partial \xi^2} + \frac{\partial^2 \phi}{\partial \eta^2} = 0$, $\frac{\partial \phi}{\partial \eta} = \frac{V}{\beta\pi} \int_0^{\infty} d\lambda \int_{-\infty}^{\infty} e^{-\lambda\eta} f'(t) \cos \lambda(t-\xi) dt$

that $\frac{\partial \phi}{\partial \eta} \rightarrow 0$ as $\eta \rightarrow \infty$ and at $\eta = 0$

$$\frac{\partial \phi}{\partial \eta} = \frac{V}{\beta\pi} \int_0^{\infty} d\lambda \int_{-\infty}^{\infty} f'(t) \cos \lambda(t-\xi) dt = \frac{V}{\beta} f'(\xi)$$

The pressure distribution may then be found from

$$c_p = -\frac{2}{V} \frac{\partial \phi}{\partial \xi} = \frac{2}{\beta\pi} \int_0^{\infty} d\lambda \int_{-\infty}^{\infty} e^{-\lambda\eta} f'(t) \sin \lambda(t-\xi) dt$$

changing the order of integration yields,

$$c_p = \frac{2}{\beta\pi} \int_{-\infty}^{\infty} f'(t) dt \int_0^{\infty} e^{-\lambda\eta} \sin \lambda(t-\xi) d\lambda$$

and integrating,

$$c_p(\xi, \eta) = \frac{2}{\beta\pi} \int_{-\infty}^{\infty} \frac{f'(t)(t-\xi)}{(t-\xi)^2 + \eta^2} dt, \text{ or in physical coordinates}$$

$$c_p = \frac{R}{\beta \pi} \int_{-\infty}^{\infty} \frac{(t-x) f'(t)}{(t-x)^2 + \beta^2 y^2} dt$$

The result can now be applied to the flow past a thin airfoil at zero angle of attack.

1. Circular arc airfoil

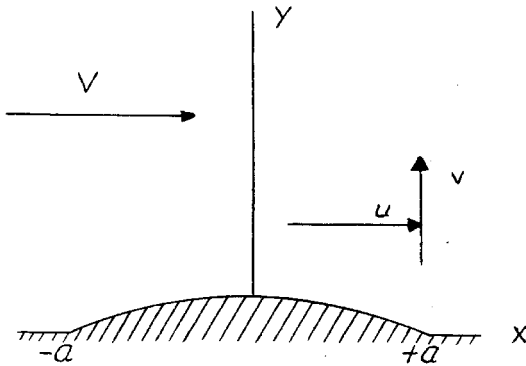
If the flow is past the circular arc airfoil shown in Fig. 3,

$$(11) \quad \begin{aligned} f'(x) &= \frac{-x}{R} & \text{for } |x| < a \\ &= 0 & \text{for } |x| > a \end{aligned}$$

to the order of the theory. Then, from (9),

$$c_p = -\frac{R}{\beta \pi R} \int_{-a}^a \frac{(t-\xi)t}{(t-\xi)^2 + y^2} dt$$

(12)



Let $a = 1$, so that integrating by parts

$$\begin{aligned} c_p &= \frac{-1}{\beta \pi R} \left[t \log(y^2 + [t-\xi]^2) \Big|_{-1}^1 - \int_{-1}^1 (y^2 + [t-\xi]^2) dt \right] \\ &= \frac{-1}{\beta \pi R} \left[\xi \log \frac{y^2 + (1-\xi)^2}{y^2 + (1+\xi)^2} + 4 \right. \\ &\quad \left. - 2y \tan^{-1} \frac{1-\xi}{y} - 2y \tan^{-1} \frac{1+\xi}{y} \right] \end{aligned}$$

or in physical coordinates

$$(13) \quad c_p(x, y) = \frac{-4}{\beta \pi R} \left[1 - \frac{x}{4} \log \frac{\beta^2 y^2 + (1+x)^2}{\beta^2 y^2 + (1-x)^2} - \frac{\beta y}{2} \left(\tan^{-1} \frac{1+x}{\beta y} + \tan^{-1} \frac{1-x}{\beta y} \right) \right]$$

Then

$$(14) \quad c_p(0, 0) = c_{p, \max} = \frac{-4}{\beta \pi R} \quad \text{approximating the surface by } y = 0,$$

and above the maximum thickness

$$(15) \quad c_p(0, y) = c_{p, \max} \left[1 - \beta y \tan^{-1} \frac{1}{\beta y} \right]$$

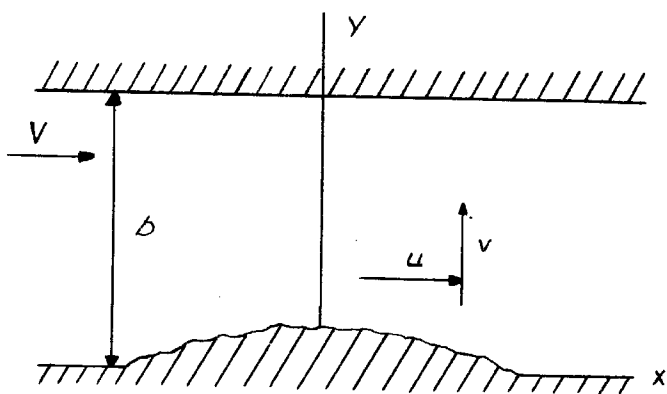
On the surface of the airfoil, or approximately at $y = 0$

$$C_p(x, 0) = C_{p0 \max} \left[1 - \frac{x}{2} \log \frac{1+x}{1-x} \right] \quad |x| < 1$$

The method of solution can now be extended to flow between boundaries.

A. Flow in a channel past a wall of arbitrary shape.

For closed channels, only the case of flow between a smooth wall and a disturbing wall will be considered but it will be obvious how flow between two disturbing walls can be built up. For the case shown in Fig. 4 the differential Eq. (8) still holds as does boundary condition 2a of (7) but boundary condition 1a must be modified so that



$$(2'a). \quad V = \frac{\partial \phi}{\partial y} = \frac{\partial \phi}{\partial \eta} \frac{1}{\beta} = 0 \text{ at}$$

$$\eta = b \quad \eta = \beta b = h \text{ say}$$

Then the solution is

$$\phi = \frac{-V}{\beta \pi} \int_0^{\infty} \frac{d\lambda}{\lambda} \int_{-\infty}^{\infty} \frac{\cosh \lambda(h-y)}{\sinh \lambda h} f'(t) \cos \lambda(t-\xi) dt$$

for

$$\nabla^2 \phi = 0 \quad \text{and}$$

$$\frac{\partial \phi}{\partial \eta} = \frac{V}{\beta \pi} \int_0^{\infty} d\lambda \int_{-\infty}^{\infty} \frac{\sinh \lambda(h-y)}{\sinh \lambda h} f'(t) \cos \lambda(t-\xi) dt \quad \text{so that}$$

$$\frac{\partial \phi}{\partial \eta} = 0 \text{ at } \eta = h \quad \text{and at } \eta = 0$$

$$\frac{\partial \phi}{\partial \eta} = \frac{V}{\beta \pi} \int_0^{\infty} d\lambda \int_{-\infty}^{\infty} f'(t) \cos \lambda(t-\xi) dt = \frac{V}{\beta} f'(\xi)$$

Then

$$(18) \quad C_p = \frac{2}{\beta\pi} \int_0^{\infty} d\lambda \int_{-\infty}^{\infty} \frac{\cosh \lambda(h-y)}{\sinh \lambda h} f(t) \sin \lambda(t-\xi) dt$$

changing the order of integration.

$$C_p = \frac{2}{\beta\pi} \int_{-\infty}^{\infty} f(t) dt \int_0^{\infty} \frac{\cosh \lambda(h-y)}{\sinh \lambda h} \sin \lambda(t-\xi) d\lambda$$

This may be integrated with respect to

$$\int_0^{\infty} \frac{\cosh \lambda \xi}{\sinh \lambda h} \sin \lambda \xi d\lambda = \frac{\pi}{2g} \frac{\sinh \frac{h\pi}{g}}{\cosh \frac{h\pi}{g} + \cos \frac{b\pi}{g}} \quad p^2 \leq g^2$$

(See Ref. 9)

Hence

$$C_p = \frac{2}{\beta\pi} \frac{\pi}{2h} \int_{-\infty}^{\infty} f(t) dt \frac{\sinh \left(\frac{t-\xi}{h} \pi \right)}{\cosh \left(\frac{t-\xi}{h} \pi \right) + \cos \left(\frac{h-y}{h} \pi \right)}$$

or

$$(19) \quad C_p(x, y) = \frac{1}{\beta^2 b} \int_{-\infty}^{\infty} \frac{\sinh \left(\frac{t-x}{\beta b} \pi \right) f(t)}{\cosh \left(\frac{t-x}{\beta b} \pi \right) - \cos \left(\frac{y}{b} \pi \right)}$$

For the case where the disturbance is restricted to $-a < x < a$, the pressure coefficient at the surface ($y = 0$) is given by

$$(20) \quad C_p(x, 0) = \frac{1}{\beta^2 b} \int_{-a}^a f(t) \coth \left(\frac{t-x}{\beta b} \pi \right) dt$$

This is identically the result obtained by Tsien and Lees in a different way (See Ref. 10). The results can now be applied to a special case.

1. Circular arc airfoil at 0° angle of attack in a wind tunnel

For this case, as before,

$$f'(z) = \frac{-z}{R} \quad \text{for } |z| < a$$

$$= 0 \quad \text{for } |z| > a$$

(See Fig. 5) Then from (18)

$$(21) \quad \phi_p(x, y) = \frac{-1}{\beta^2 b R} \int_{-a}^a \frac{t \operatorname{cosh}\left(\frac{t-x}{\beta b} \pi\right)}{-\alpha \operatorname{cosh}\left(\frac{t-x}{\beta b} \pi\right) - \cos\left(\frac{y}{b} \pi\right)} dt$$

Now let

$$a = 1$$

$$\frac{t\pi}{h} = \frac{t\pi}{\beta b} = p$$

$$\frac{y\pi}{h} = \frac{y\pi}{\beta b} = q$$

$$\bar{y} = \frac{y}{b}$$

$$\frac{\pi}{h} = \frac{\pi}{\beta b} = \mu = \frac{\alpha}{\beta} ; \quad \alpha = \frac{\pi}{b}$$

Then

$$\phi_p = \frac{-1}{\beta^2 b R} \frac{h^2}{\pi^2} \int_{-\mu}^{\mu} \frac{p \operatorname{cosh}(p-q)}{\operatorname{cosh}(p-q) - \cos \pi \bar{y}} dp$$

or

$$(22) \quad \phi_p = \frac{-1}{\pi R \alpha} \int_{-\mu}^{\mu} \frac{p \operatorname{cosh}(p-q)}{\operatorname{cosh}(p-q) - \cos \pi \bar{y}} dp$$

This can easily be evaluated at the surface of the airfoil ($\bar{y} = 0$),

for

$$(23) \quad \phi_p(x, 0) = \frac{-1}{\pi R \alpha} \int_{-\mu}^{\mu} p \operatorname{cosh}\left(\frac{p-x}{2}\right) dp$$

Now
$$\coth\left(\frac{p-g}{2}\right) = \frac{2}{p-g} \left\{ 1 + \sum_{n=1}^{\infty} \frac{(-1)^{n-1}}{(2n)!} \frac{2^{2n} B_{2n-1}}{(p-g)^{2n}} \right\} \left(\frac{p-g}{2}\right)^{2n}$$

where the B_K are Bernoulli numbers.

This converges everywhere for a worst case of $b = \frac{1}{2\beta}$. For a narrower channel other forms of expansion may be used, as for example in Ref. 3, but this is sufficient for very practical cases.

Hence
$$c_p(x,0) = \frac{-2}{\pi R \alpha} \int_{-\mu}^{\mu} \frac{p}{p-g} dp - \frac{2}{\pi R \alpha} \sum_{n=1}^{\infty} \frac{(-1)^{n-1}}{(2n)!} \frac{B_{2n-1}}{(p-g)^{2n}} \int_{-\mu}^{\mu} (p-g)^{2n-1} p dp$$

or

(24)
$$c_p(x,0) = \frac{-4}{\pi R \beta} \left[1 - \frac{x}{2} \log \left| \frac{1+x}{1-x} \right| \right] - \frac{2}{\pi R \alpha} \sum_{n=1}^{\infty} \frac{(-1)^{n-1}}{(2n)!} \frac{B_{2n-1}}{(p-g)^{2n}} \int_{-\mu}^{\mu} (p-g)^{2n-1} p dp$$

It is seen that the first term of (24) corresponds to a surface distribution of pressure (c_{p_0}) without a tunnel wall (Eq. 16), and the second term gives the interference effects.

i.e. (24)
$$c_p(x,0) = c_{p0} + \Delta c_p(x,0)$$

where
$$\Delta c_p(x,0) = \frac{-2}{\pi R \alpha} \sum_{n=1}^{\infty} \frac{(-1)^{n-1}}{(2n)!} \frac{B_{2n-1}}{(p-g)^{2n}} \int_{-\mu}^{\mu} (p-g)^{2n-1} p dp$$

But
$$\int_{-\mu}^{\mu} p(p-g)^{2n-1} dp = \frac{p(p-g)^{2n}}{2n} \Big|_{-\mu}^{\mu} - \int_{-\mu}^{\mu} \frac{(p-g)^{2n}}{2n} dp$$

$$= \frac{(g+2n\mu)(\mu-g)^{2n} - (g-2n\mu)(\mu+g)^{2n}}{2n(2n+1)}$$

Hence,

(26)
$$\Delta c_p(x,0) = \frac{-2}{\pi R \beta} \sum_{n=1}^{\infty} \frac{(-1)^{n-1}}{(2n+1)!(2n)} \frac{B_{2n-1}}{(p-g)^{2n}} \left[(x+2n)(1-x)^{2n} - (x-n)(1+x)^{2n} \right]$$

and for $x = 0$

$$\Delta C_{p, \max} = C_{p, \max} \sum_{n=1}^{\infty} (-1)^{n-1} \frac{B_{2n-1}}{(2n+1)!} \left(\frac{\alpha}{\beta}\right)^{2n} \quad \text{where } C_{p, \max} = \frac{-4}{\beta \pi R}$$

or

$$(27) \quad C_p(x, 0) = C_{p, \max} \left[1 + \sum_{n=1}^{\infty} (-1)^{n-1} \frac{B_{2n-1}}{(2n+1)!} \left(\frac{\alpha}{\beta}\right)^{2n} \right]$$

The c_p can also be easily obtained at the tunnel wall $\bar{y} = 1$. From (22)

$$(28) \quad C_p(x, b) = \frac{-1}{\pi R \alpha} \int_{-\mu}^{\mu} p \tanh\left(\frac{p-g}{2}\right) dp.$$

But

$$\tanh\left(\frac{p-g}{2}\right) = \sum_{n=1}^{\infty} (-1)^{n-1} \frac{2^{2n} (2^{2n} - 1)}{(2n)!} \left(\frac{p-g}{2}\right)^{2n-1} \quad \text{for } \left(\frac{p-g}{2}\right)^2 < \frac{\pi^2}{4}$$

Then proceeding as before we get

$$(29) \quad C_p(x, b) = \frac{-1}{\pi R \beta} \sum_{n=1}^{\infty} (-1)^{n-1} \frac{2^{2n} (2^{2n} - 1) B_{2n-1}}{n(2n+1)!} \left[(x+2n)(1-x)^{2n} - (x-2n)(1+x)^{2n} \right] \left(\frac{\alpha}{\beta}\right)^{2n}$$

and at $x = 0$ or above the maximum thickness

$$(30) \quad C_p(0, b) = C_{p, \max} \sum_{n=1}^{\infty} (-1)^{n-1} \frac{2^{2n} (2^{2n} - 1) B_{2n-1}}{(2n+1)!} \left(\frac{\alpha}{\beta}\right)^{2n}$$

Another place where c_p may be easily found is $\bar{y} = 1/2$ or half way

between the wall and airfoil. Then from (22)

$$(31) \quad C_p(x, b/2) = \frac{-1}{\pi R \alpha} \int_{-\mu}^{\mu} p \tanh(p-g) dp$$

so that

$$C_p(x, b/2) = \frac{-1}{\pi R \beta} \sum_{n=1}^{\infty} (-1)^{n-1} \frac{2^{2n} (2^{2n} - 1) B_{2n-1}}{2n(2n+1)!} \left[(x+2n)(1-x)^{2n} - (x-2n)(1+x)^{2n} \right] \left(\frac{\alpha}{\beta}\right)^{2n}$$

or

$$(32) \quad C_p(0, b/2) = \frac{-2}{\pi R \beta} \sum_{n=1}^{\infty} (-1)^{n-1} \frac{2^{2n} (2^{2n} - 1)}{(2n+1)!} B_{2n-1} \left(\frac{\alpha}{\beta} \right)^{2n}$$

$$C_p(0, b/2) = C_{p, \text{max}} \sum_{n=1}^{\infty} (-1)^{n-1} \frac{2^{2n-1} (2^{2n} - 1)}{(2n+1)!} B_{2n-1} \left(\frac{\alpha}{\beta} \right)^{2n}$$

This last solution may be extended by a Taylor expansion, by putting

$$(33) \quad C_p(0, y) = C_p(0, b/2) + (y - b/2) C_p'(0, b/2) + \frac{(y - b/2)^2}{2!} C_p''(0, b/2) + \dots$$

when $C_p' = \frac{\partial C_p}{\partial y}$ etc.

From (21) we have,

$$(34) \quad C_p(0, y) = \frac{-2}{\pi R \alpha} \int_0^{\mu} \frac{\mu \sin h \mu}{\cosh \mu - \cos \pi y} d\mu$$

Hence,

$$C_p'(0, y) = \frac{2}{\pi R \alpha} \int_0^{\mu} \frac{\mu \sin h \mu}{(\cosh \mu - \cos \pi y)^2} \left(\frac{\pi}{b} \right) \sin \pi y d\mu$$

$$C_p'(0, b/2) = \frac{2}{\pi R \alpha} \int_0^{\mu} \left(\frac{\pi}{b} \right) \frac{\mu \sin h \mu}{\cosh^2 \mu} d\mu$$

$$(35) \quad = \frac{2}{\pi R \alpha} \left(\frac{\pi}{b} \right) \left[-\frac{\mu}{\cosh \mu} \Big|_0^{\mu} + \int_0^{\mu} \frac{d\mu}{\cosh \mu} \right]$$

so

$$(36) \quad C_p'(0, b/2) = \frac{2}{\pi R \alpha} \left[\tan^{-1}(\sinh \mu) - \frac{\mu}{\cosh \mu} \right] \left(\frac{\pi}{b} \right)$$

Then

$$C_p''(0, y) = \frac{2}{\pi R \alpha} \int_0^{\mu} \left(\frac{\pi}{b} \right)^2 \mu \sin h \mu \left[\frac{\cos \pi y}{(\cosh \mu - \cos \pi y)^2} - \frac{2 \sin^2 \pi y}{(\cosh \mu - \cos \pi y)^3} \right] d\mu$$

and

$$c_p''(0, b/2) = \frac{2}{\pi R \alpha} \left(\frac{\pi}{b}\right)^2 \int_0^{\mu} \left(\frac{-2 \sinh \frac{\mu}{2}}{\cosh^2 \frac{\mu}{2}}\right) \mu \, d\mu.$$

15.

$$= \frac{2}{\pi R \alpha} \left(\frac{\pi}{b}\right)^2 \left[\frac{\mu}{\cosh^2 \frac{\mu}{2}} \Big|_0^{\mu} - \int_0^{\mu} \frac{d\mu}{\cosh^2 \frac{\mu}{2}} \right]$$

or

$$(37) \quad c_p''(0, b/2) = \frac{2}{\pi R \alpha} \left(\frac{\pi}{b}\right)^2 \left[\tanh \frac{\mu}{2} - \frac{\mu}{\cosh^2 \frac{\mu}{2}} \right]$$

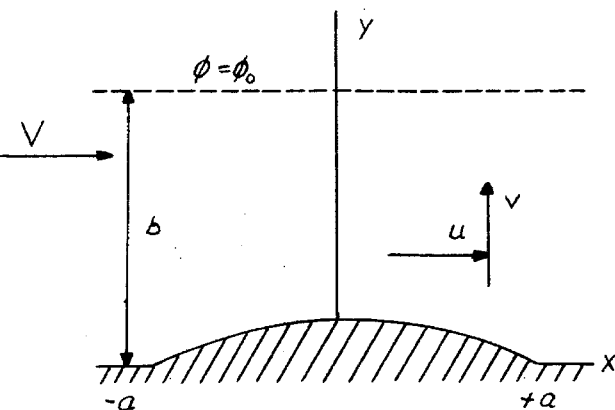
Then from (32) and (33)

$$c_p(0, y) = \frac{-2}{\pi R \alpha} \left\{ \sum_{n=1}^{\infty} \frac{(-1)^{n-1} 2^{2n} (2^{2n} - 1)}{(2n+1)!} B_{2n-1} \left(\frac{\alpha}{\beta}\right)^{2n+1} - \left(\frac{\pi}{b}\right)(y - b/2) \left[\tan^{-1} \left(\sinh \frac{\alpha}{\beta} \right) - \frac{\alpha}{\beta \cosh \frac{\alpha}{\beta}} \right] - \frac{1}{2} \left(\frac{\pi}{b}\right)^2 (y - b/2)^2 \left[\tanh \frac{\alpha}{\beta} - \frac{\alpha}{\beta \cosh^2 \frac{\alpha}{\beta}} \right] + \dots \right\}$$

$$(38) \quad c_p(0, y) = c_{p, \text{pert}} \left\{ \sum_{n=1}^{\infty} \frac{(-1)^{n-1} 2^{2n-1} (2^{2n} - 1)}{(2n+1)!} B_{2n-1} \left(\frac{\alpha}{\beta}\right)^{2n} + \frac{\pi \beta}{2 \alpha} \left(\frac{1}{2} - \bar{y}\right) \left[\tan^{-1} \left(\sinh \frac{\alpha}{\beta} \right) - \frac{\alpha}{\beta \cosh \frac{\alpha}{\beta}} \right] - \frac{\pi^2}{2} \left(\frac{\beta}{2 \alpha}\right) \left(\frac{1}{2} - \bar{y}\right)^2 \left[\tanh \frac{\alpha}{\beta} - \frac{\alpha}{\beta \cosh^2 \frac{\alpha}{\beta}} \right] + \dots \right\}$$

For the case when the disturbing wall is in a jet, or the airfoil is in an open wind tunnel, the same method can be applied. For the flow as in Fig. 5a the boundary condition 2'a must be changed so that

(2'' a $\phi = \phi_0$ a constant at $y = b$ or $y = h$), but otherwise the problem is the same. Hence, the solution can be written.



$$(39) \quad \phi = \frac{-V}{\beta\pi} \int_0^{\infty} \frac{d\lambda}{\lambda} \int_{-\infty}^{\infty} \frac{\sinh \lambda(h-y)}{\cosh \lambda h} f(t) \cos \lambda(t-\xi) dt + \phi_0$$

for then

$$\frac{\partial^2 \phi}{\partial \xi^2} + \frac{\partial^2 \phi}{\partial y^2} = 0, \quad \phi = \phi_0 \quad \text{at } y=h, \quad y=0$$

$$\frac{\partial \phi}{\partial y} = \frac{V}{\beta\pi} \int_0^{\infty} d\lambda \int_{-\infty}^{\infty} f(t) \cos \lambda(t-\xi) dt = \frac{V}{\beta} f'(\xi).$$

Then, in the same way as before,

$$(40) \quad C_p = \frac{2}{\beta\pi} \int_0^{\infty} d\lambda \int_{-\infty}^{\infty} \frac{\sinh \lambda(h-y)}{\cosh \lambda h} f'(t) \sin \lambda(t-\xi) dt$$

or changing the order of integration

$$C_p = \frac{2}{\beta\pi} \int_{-\infty}^{\infty} f'(t) dt \int_0^{\infty} \frac{\sinh \lambda(h-y)}{\cosh \lambda h} \sin \lambda(t-\xi) d\lambda$$

But $\int_0^{\infty} \frac{\sinh \frac{p\pi}{b} w}{\cosh \frac{p\pi}{b} w} \sin \pi w dw = \frac{\pi}{b} \sin \frac{p\pi}{2b} \frac{\sinh \frac{k\pi}{2q}}{\cosh \frac{k\pi}{b} + \cos \frac{p\pi}{q}}$ see 29

See Ref. 2

so that

$$(41) \quad C_p(x,y) = \frac{2}{\beta^2 b} \sin \left[\frac{\pi}{2} \left(1 - \frac{y}{b} \right) \right] \int_{-\infty}^{\infty} \frac{f'(t) \sinh \left(\frac{t-x}{\beta b} \frac{\pi}{2} \right)}{\cosh \left(\frac{t-x}{\beta b} \pi \right) - \cos \frac{y}{b} \pi} dt.$$

These results can be applied to the same disturbance as before.

2. Circular arc airfoil in open wind tunnel.

Then in the same notation as before

$$(42) \quad C_p = \frac{-2}{\beta^2 b R} \sin \left[\frac{\pi}{2} (1 - \bar{y}) \right] \int_{-1}^1 \frac{t \sinh \left(\frac{t-x}{\beta b} \frac{\pi}{2} \right)}{\cosh \left(\frac{t-x}{\beta b} \pi \right) - \cos \pi \bar{y}} dt.$$

$$C_p = \frac{-2}{\beta^2 b R} \sin \left[\frac{\pi}{2} (1 - \bar{y}) \right] \frac{k^2}{\pi^2} \int_{-\mu}^{\mu} \frac{p \operatorname{snh} \left(\frac{k-p}{2} \right)}{\operatorname{cosh}(p-q) - \cos \pi \bar{y}} dp.$$

17.

and a special case of some interest is $x = y = 0$. Then

$$C_p(0,0) = -\frac{4}{\pi R \beta} \int_0^{\mu} \frac{p \operatorname{snh} \frac{k}{2}}{\operatorname{cosh} p - 1} dp$$

(43)

$$= C_{p_{\max}} \int_0^{\mu} \frac{k}{2} \operatorname{cosh} \frac{k}{2} dp$$

Expanding

$$\operatorname{cosh} \frac{k}{2} = \frac{2}{p} \left[1 + 2 \sum_{n=1}^{\infty} (-1)^n \frac{(2^{n-1} - 1) B_{2n-1}}{(2n)!} \left(\frac{k}{2} \right)^{2n} \right]$$

and integrating yields

$$C_p = C_{p_{\max}} \left[1 + 2 \sum_{n=1}^{\infty} (-1)^n \frac{(2^{n-1} - 1) B_{2n-1}}{2^{2n} (n+1)!} \left(\frac{\alpha}{\beta} \right)^{2n} \right]$$

so that

$$(44) \quad C_p(0,0) = C_{p_{\max}} \left[1 + 2 \sum_{n=1}^{\infty} (-1)^n \frac{(2^{n-1} - 1) B_{2n-1}}{2^{2n-1} (n+1)!} \left(\frac{\alpha}{\beta} \right)^{2n} \right].$$

II RESULTS AND COMPARISON WITH EXPERIMENTS

Some results and comparison with experiments are shown in Figs. 6-13. The experiments were made in the 2" x 20" transonic wind tunnel of the GALCIT (see Ref. 11).

Figs. 6 and 7 show the pressure distribution at the airfoil surface. $C_{p\text{critical}}$ denotes pressure at which $M = 1$. As would be expected, the agreement is better in the leading half of the airfoil and at lower Mach numbers. There is intrinsically less error in the theory at lower Mach numbers. Also, boundary layer effects in distorting the shape of the surface are less at smaller Mach numbers and on the leading part of the airfoil. The effect of boundary layer and occurrence of shock waves on the aft part of the airfoil have been noted in schlieren photographs (see Ref. 13). The parameters used in the computation were

$$a = \text{half chord of airfoil} = 1.5" = 1$$

$$R = \text{radius of curvature of airfoil surface} = 6.785 = 4.51$$

$$b = 1/2 \text{ height of tunnel} = 10" = 6.67$$

$$\alpha = \frac{\pi}{b} \text{ tunnel height parameter} = \frac{\pi}{6.67} = .471.$$

It was interesting to note that the wall interference effect was approximately constant along the surface of the airfoil when computed with these parameters.

Fig. 8 makes some comparison of the wind tunnel wall effects for this tunnel and shows especially the increasing effect at higher M . It is noted that the interference effect of an open wind tunnel is less than that of a closed one. Fig. 9 shows how strongly

the ratio of tunnel height to model chord affects the interference. Fig. 10 gives some indication of the decay of airfoil disturbance above the surface. It also indicates that the supersonic region predicted would be too small.

In order to get the shape of some typical supersonic regions Figs. 11, 12, 13 were prepared and for simplicity wind tunnel wall effects were neglected. To show how much the local supersonic zone computed differs from the supersonic flow, the distribution of velocity on the supersonic zone at the surface was used as a starting point and the flow field extended by the method of characteristics (See Ref. 3). The result is shown as the dotted line in Fig. 11. Actually, the supersonic zones in this airfoil become more asymmetric at higher M and hence the agreement with potential theory would be worse.

An interesting theoretical method to determine conditions within the supersonic zone would be to successively alter the surface distribution of pressure in the supersonic zone and make the $M = 1$ boundary of the characteristic extension agree with that predicted by the small perturbation theory.

The small perturbation theory has then yielded some interesting results for transonic flow over airfoils, but for more information more accurate theories are needed. It is felt that the best attacks in the future will be through the second approximation of this theory or through the approximate transonic equation.

REFERENCES

1. Taylor, G. I., "The Flow of Air at High Speeds Past Curved Surfaces". R. & M. 1381 January 1930.
2. Gortler, H., "Zum Ubergang von Unterschall-zu Überschallgeschwindigkeiten in Dusen". Z.A.M.M. Vol. 19, 1939, pp. 325-337.
3. Liepmann, H. W., and Puckett, A., "The Aerodynamics of Compressible Fluids". John Wiley and Sons, 1946.
4. Tsien, H.S., and Kuo, Y. H., "Two-Dimensional Irrotational Mixed Subsonic and Supersonic Flow of a Compressible Fluid and the Upper Critical Mach Number". GALCIT Report to NACA under contract No. NAW 2793, Dec. 15, 1944 - Restricted.
5. Hentsche, W., and Wendt, H., "Die Kompressible Potential Stroemung um eine Schar von nicht angestellten symmetrische Zylinder im Kanal". LFF, Vol. 18, pp. 311-316, 1941, also NACA Tech. Memo. 1030, 1942.
6. Lamb, H., "Hydrodynamics". Cambridge University Press 1932.
7. Bateman, H., "Notes on a Differential Equation which occurs in the Two-Dimensional Motion of a Compressible Fluid and the Associated Variational Problems". Proc. Roy. Soc. A Vol. 125, pp. 598-616 1929.
8. Gortler, H., Zeit. f. Angew. Math. u. Mech. 20 (1940) pp. 254-262.
9. Haan, Bierens de, Table of Definite Integrals, Table 265.
10. Tsien, H. S., and Lees, L., "The Glauert-Prandtl Approximation for Subsonic Flows of a Compressible Fluid". J. Ae. Sci., Vol. 12, 1945.
11. Liepmann, H. W., "The 2" x 20" Transonic Wind Tunnel". GALCIT Report to AAF Materiel Command under Contract No. W 33-038 ac1717 (11592)
12. Liepmann, H. W., "Investigations of the Interaction of Boundary Layer and Shock Waves in Transonic Flow". GALCIT Report to AAF Materiel Command under Contract No. W 33-038 ac-1717 (11592)

FIG. 5

COMPARISON OF EXPERIMENTAL DATA
AND COMPUTED PRESSURE DISTRIBUTION
INCLUDING WALL EFFECT

3" x 12% CIRCULAR ARC AIRFOIL
 $M_{\infty} = 0.795$

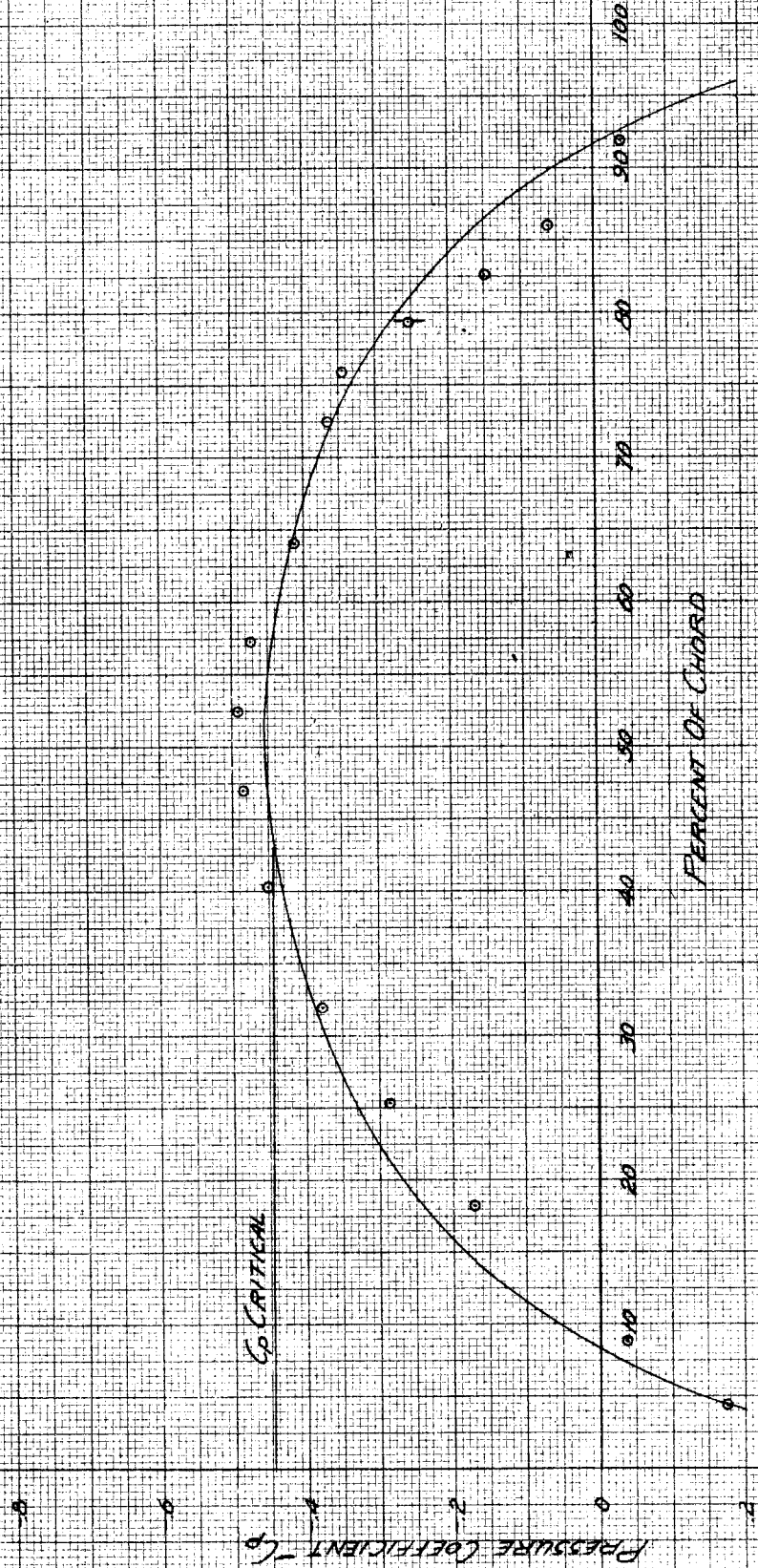


FIG. 7

COMPARISON OF EXPERIMENTAL DATA AND
COMPUTED PRESSURE DISTRIBUTION
INCLUDING WALL EFFECT

3 1/2% CIRCULAR ARC AIRFOIL
 $M_\infty = 0.845$

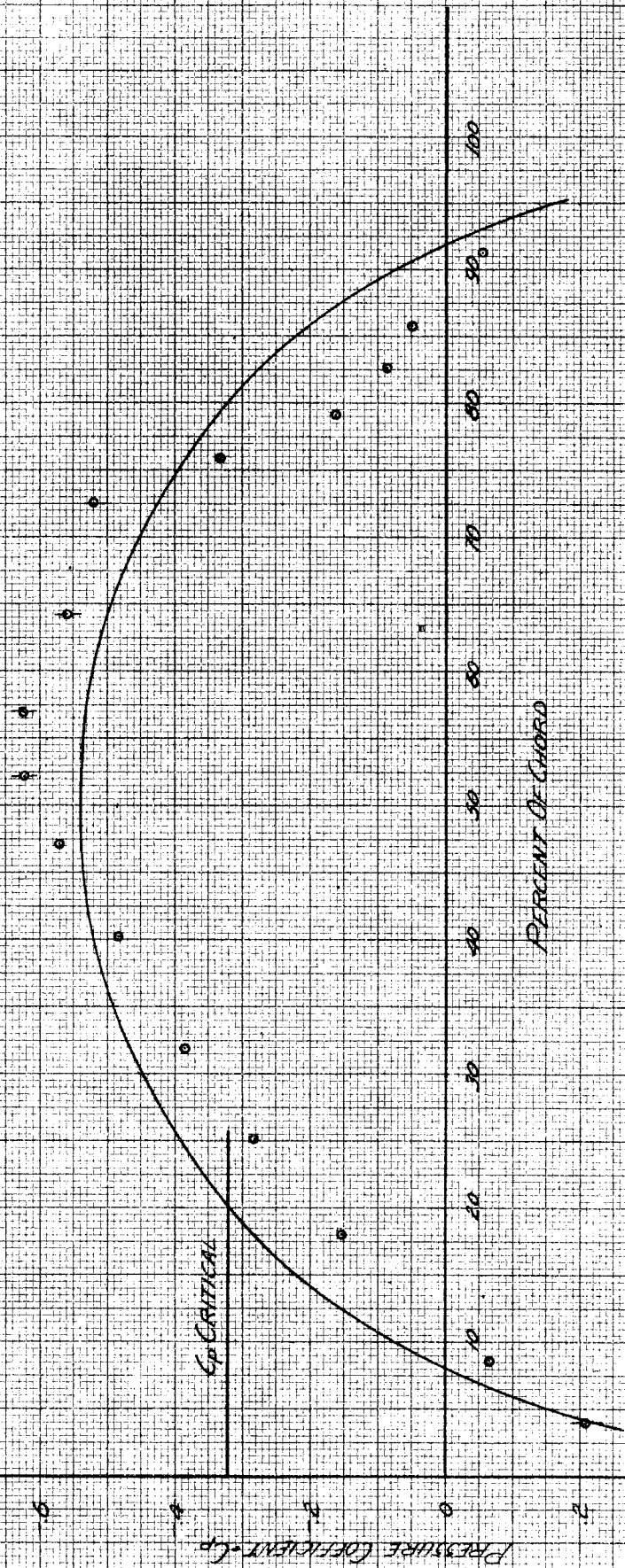
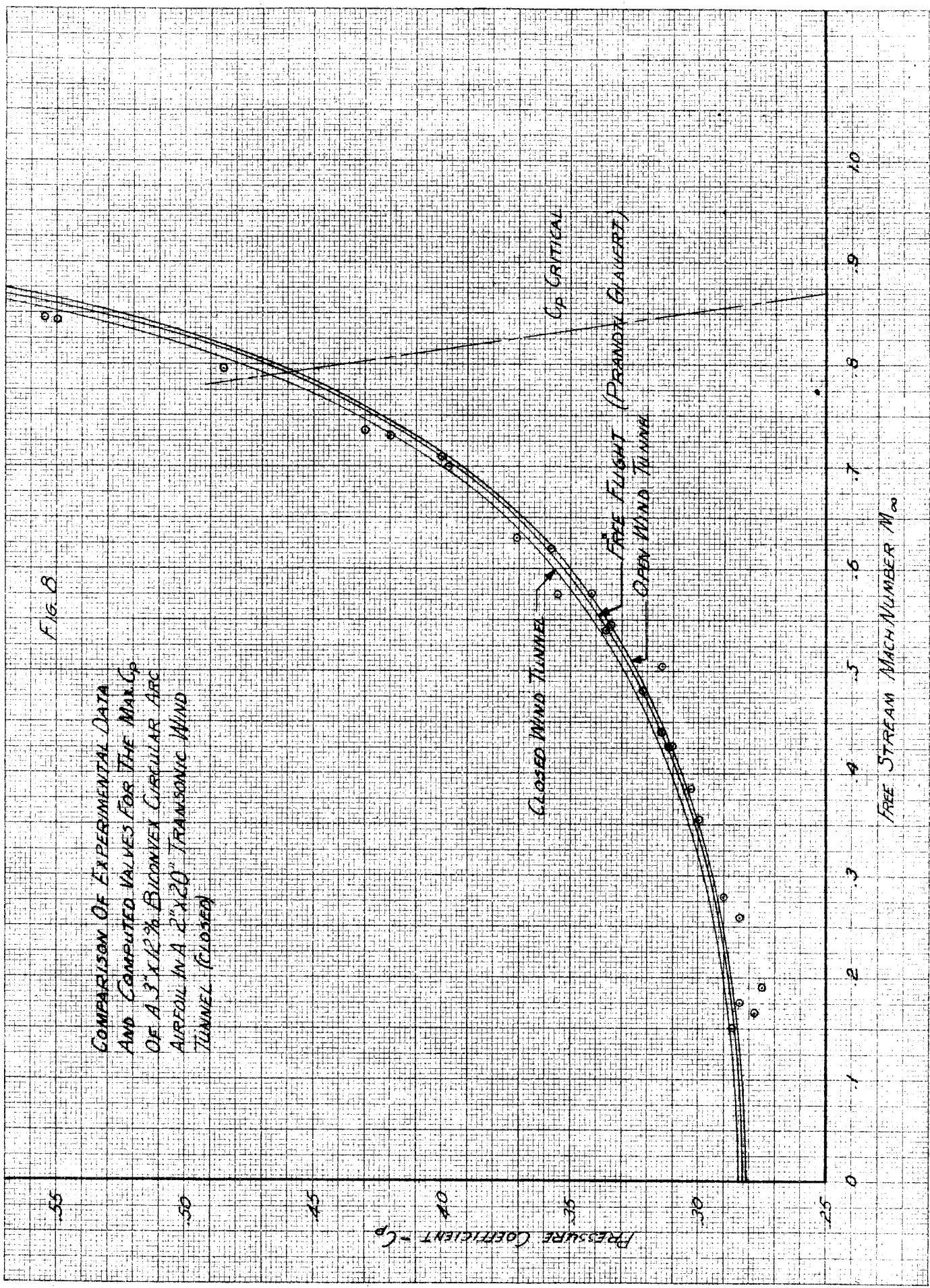


FIG. 8

COMPARISON OF EXPERIMENTAL DATA
AND COMPUTED VALUES FOR THE C_p
OF A 3' X 12 1/2' BICONVEX CIRCULAR ARC
AIRFOIL IN A 2' X 20" TRANSONIC WIND
TUNNEL (CLOSED)



FREE STREAM MACH NUMBER M_∞

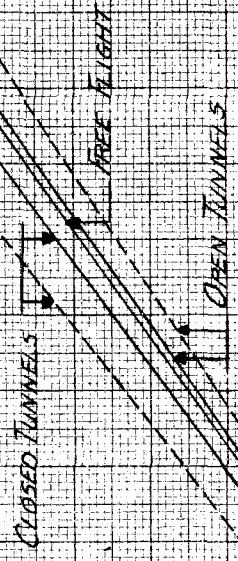
PRESSURE COEFFICIENT - C_p

FIG. 9

EFFECT OF WIND TUNNEL INTERFERENCE ON THE MAX. C_p OF A $3 \times 12 \frac{1}{2}$ CIRCULAR ARC AIRFOIL IN A 2" X 20" WIND TUNNEL

RATIO OF TUNNEL HEIGHT TO MODEL CHORD:

— 0.67
 - - - 3.33



55

50

45

40

35

30

25

$-C_p$ PRESSURE COEFFICIENT

10

11

12

13

14

15

16

17

18

19

20

COMPRESSIBILITY PARAMETER

$$\frac{1}{\sqrt{1-M^2}} = \frac{1}{\rho}$$

FIG. 10

COMPARISON OF EXPERIMENTAL DATA
AND COMPUTED VALUES ABOVE MAX.
AIRFOIL THICKNESS
 $M_\infty = 0.846$

— INCLUDES WALL EFFECT
- - - WITHOUT WALL

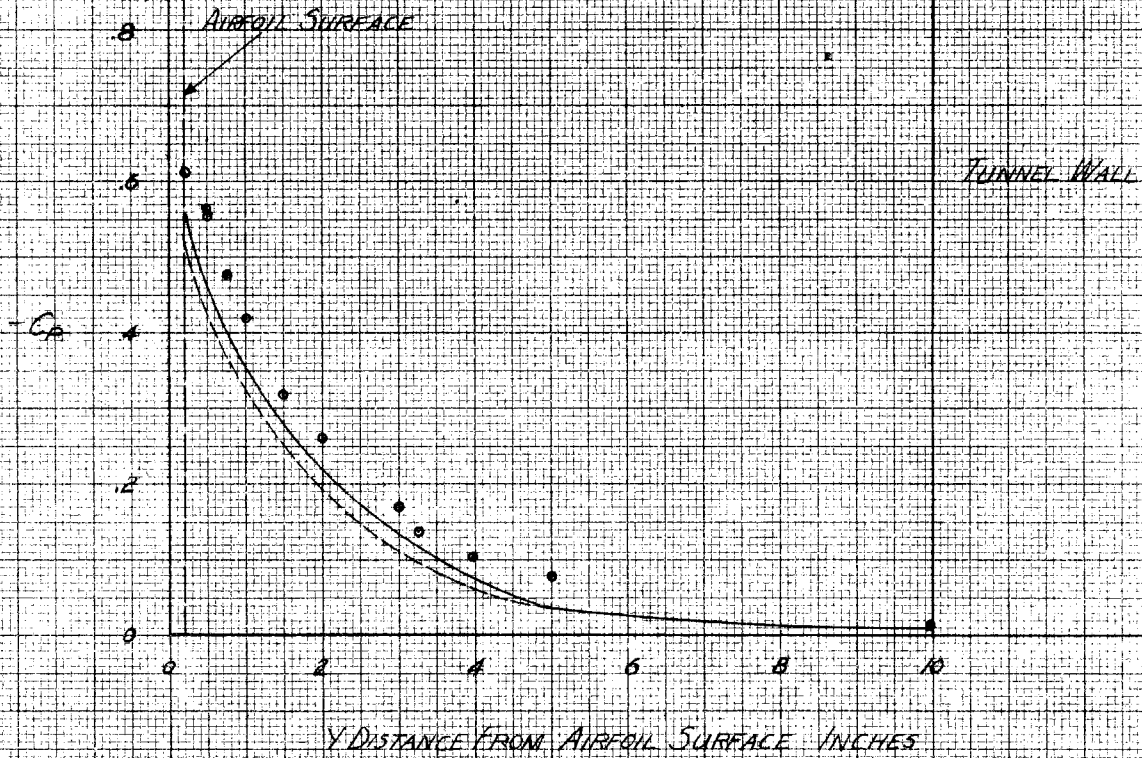
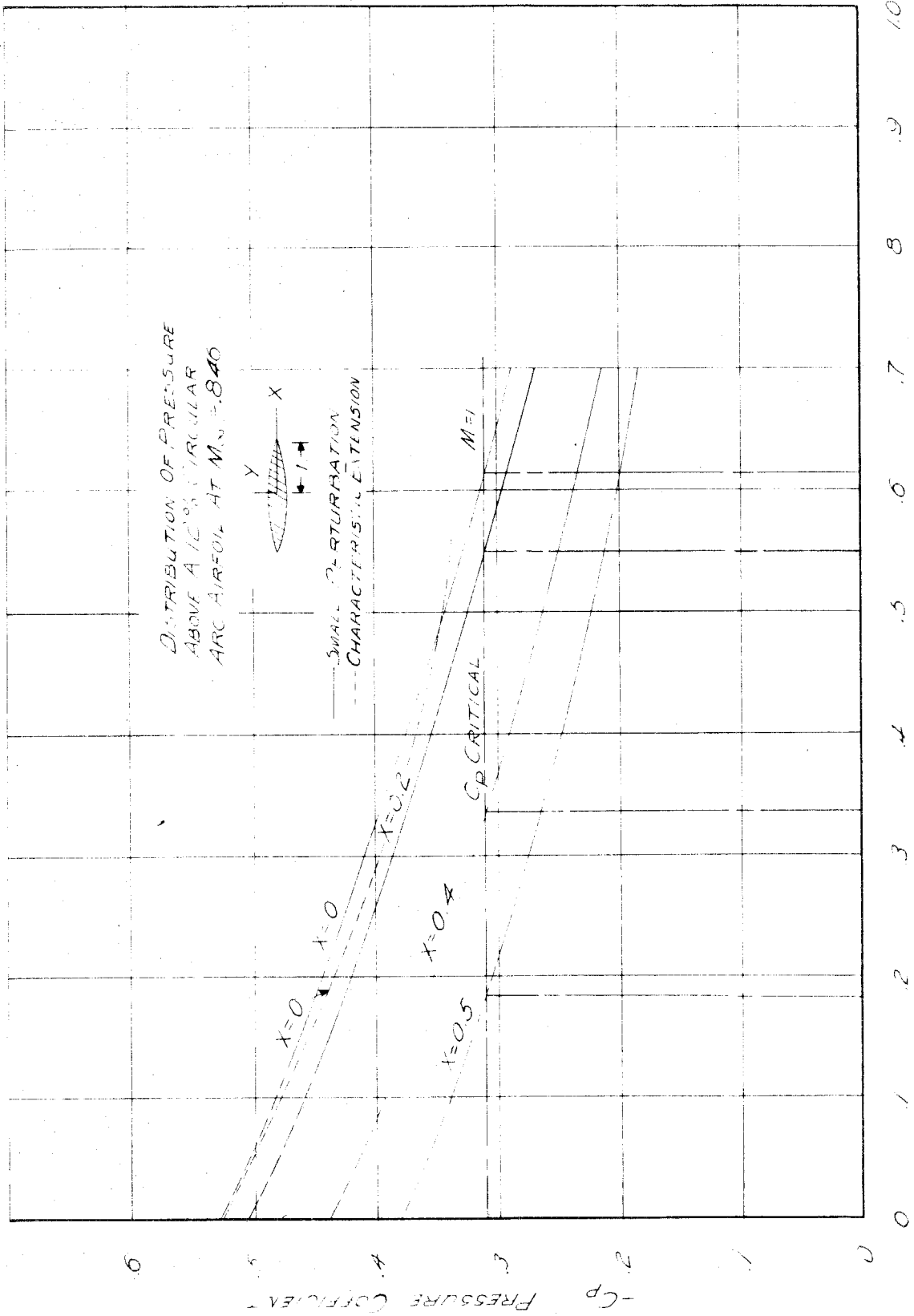


Fig. 11



x DISTANCE FROM LEADING EDGE OF AIRFOIL NORMAL TO FLOW

M=1 FOR $M_\infty = 8.56$

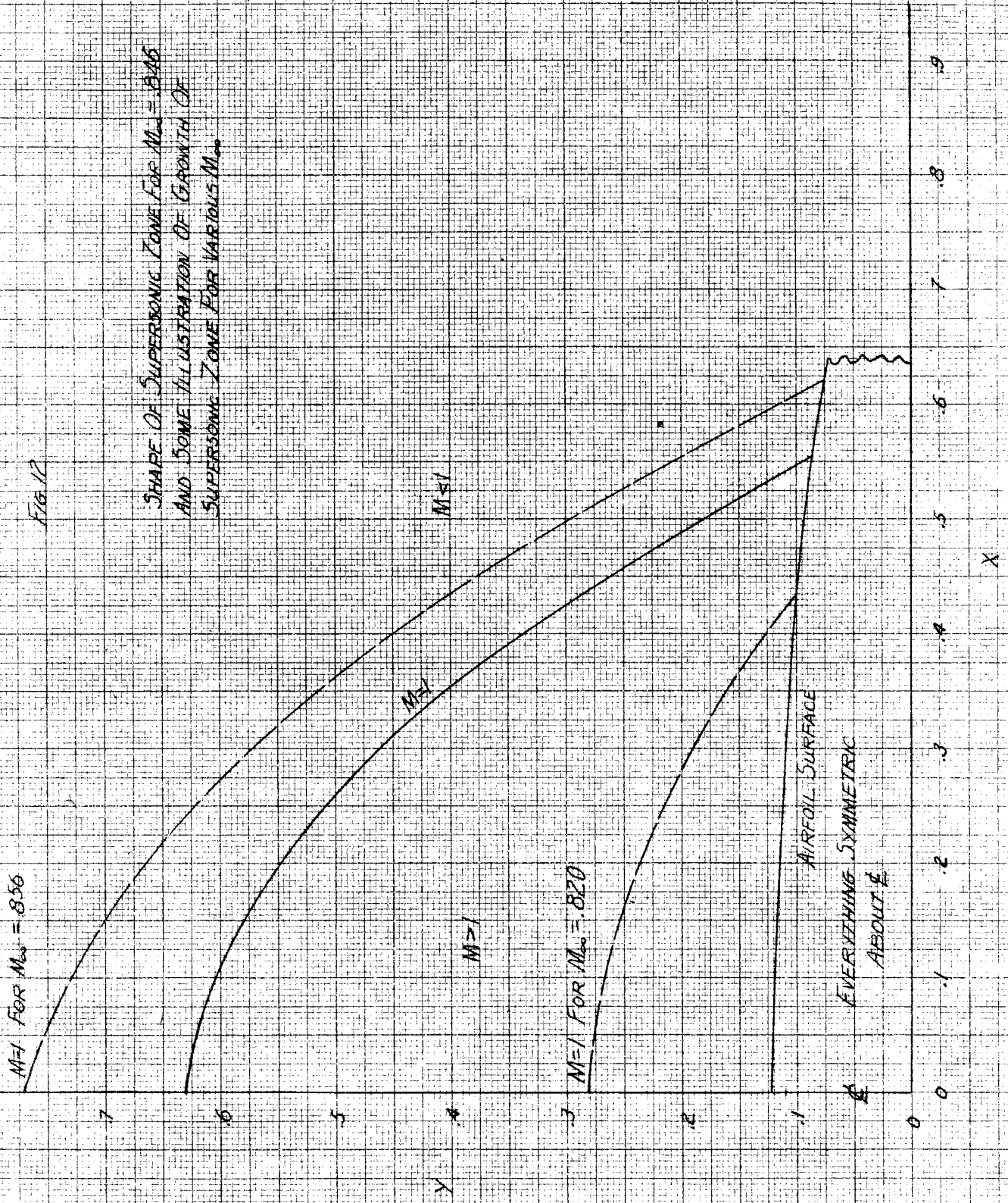


FIG. 12

SHAPE OF SUPERSONIC ZONE FOR $M_\infty = 8.56$
AND SOME ILLUSTRATION OF GROWTH OF
SUPERSONIC ZONE FOR VARIOUS M_∞

PERCENT OF HALF CHORD
X

Y

M=1 FOR $M_\infty = 8.20$

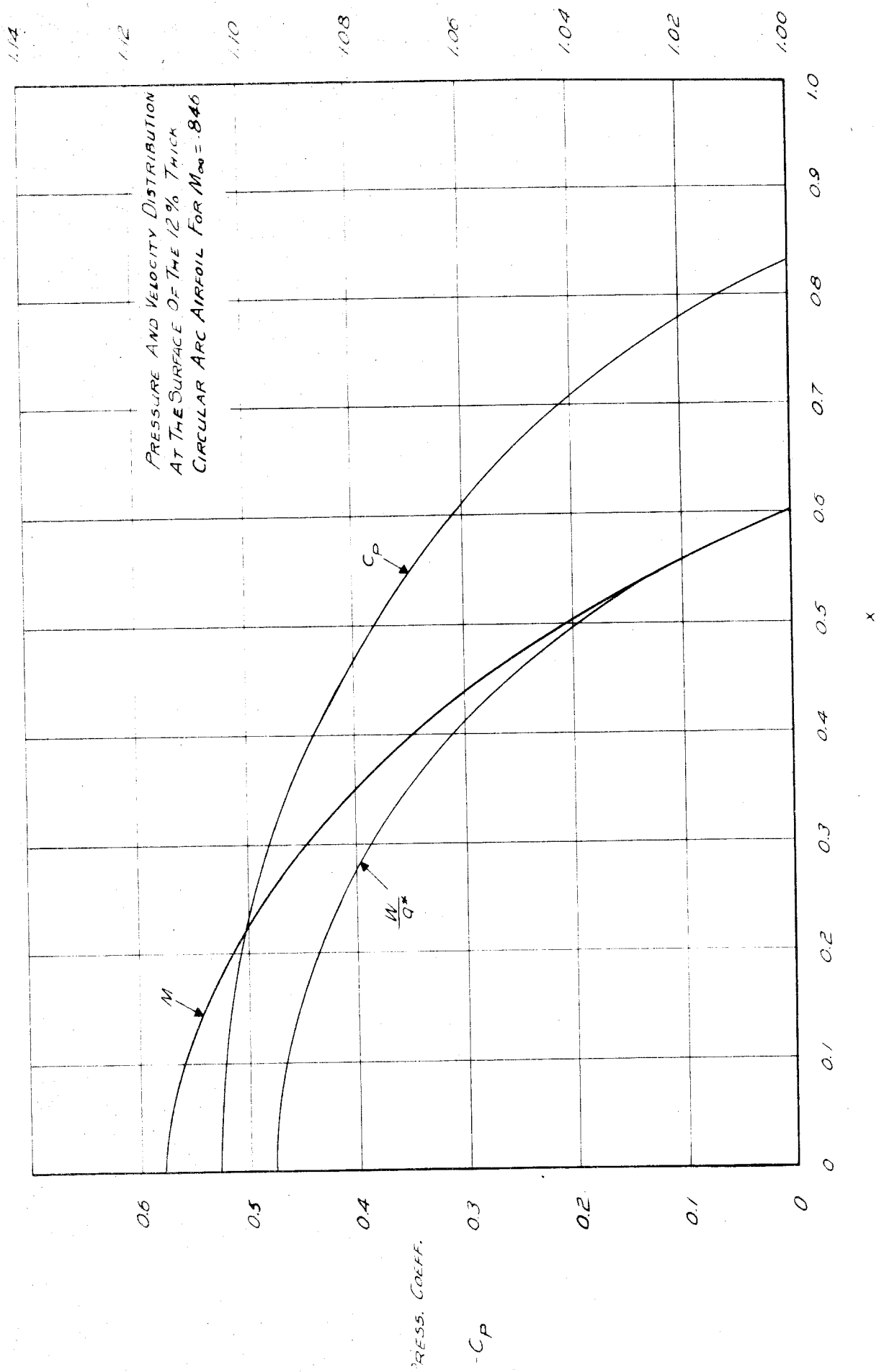
M=1

M=1

AIRFOIL SURFACE

EVERYTHING SYMMETRIC
ABOUT X

FIG. 13



DISTANCE FROM MAX. THICKNESS $C=2$